THE ASTROPHYSICAL JOURNAL, 554:L000–L000, 2001 June 20
© 2001. The American Astronomical Society. All rights reserved. Printed in U.S.A.

A PHASE-CONNECTED BRAKING INDEX MEASUREMENT FOR THE LARGE MAGELLANIC CLOUD PULSAR PSR B0540−69

W. ZHANG,[1] F. E. MARSHALL,[1], E. V. GOTTHELF,[2] J. MIDDLEDITCH,[3] AND Q. D. WANG[4]

Received 2001 February 22; accepted 2001 May 11; published 2001 June 12

ABSTRACT

We report the results of an extensive monitoring campaign of PSR B0540−69, the 50 ms pulsar in the Large Magellanic Cloud, using data acquired with the *Rossi X-Ray Timing Explorer*. A set of 45 pointed X-ray observations spanning 1.2 yr reveals a steady spin-down interrupted by a single glitch event, the first recorded for this young, rotation-powered pulsar. The quality of the data allowed us to perform a pulse-timing analysis that successfully maintains cycle count between observations, after allowing for the observed glitch. The glitch event occurred on MJD 51,325 ± 45 (90% CL error) and is characterized by a change in frequency of $\Delta\nu/\nu = (1.90 \pm 0.04) \times 10^{-9}$ and in frequency derivative of $\Delta\dot{\nu}/\dot{\nu} = (8.5 \pm 0.5) \times 10^{-5}$. By phase-linking the data set we provide a definitive measurement of the spin frequency of the pulsar and its first and second derivatives. These translate into a braking index of $n = 1.81 \pm 0.07$, significantly lower than reported previously for this source using measurements that could not be phase-linked unambiguously.

Subject headings: pulsars: individual (PSR B0540−69) — stars: neutron — X-rays: stars

1. INTRODUCTION

The young 50 ms X-ray pulsar PSR B0540−69 in N158A is one of two examples of a Crab-like pulsar in the LMC (Seward, Harnden, & Helfand 1984; Marshall et al. 1998). Like the Crab, this energetic pulsar is contained within a bright synchrotron wind nebula, i.e., a "plerion," emitting in the X-ray, optical, and radio wave bands, indicative of a rotation-powered pulsar (Middleditch & Pennypacker 1985; Manchester et al. 1993). For such isolated systems, external torques will gradually slow down the pulsar's rotation via conversion of rotational energy into electromagnetic radiation and/or a particle wind. Such a wind is thought to energize the observed plerion. PSR B0540−69 has a characteristic spin-down age ($-\nu/2\dot{\nu}$) of 1670 yr and an energy loss rate of $\dot{E} = (2\pi)^2 I\nu\dot{\nu} \simeq 1.5 \times 10^{38} I_{45}$ ergs s^{-1}, where I_{45} is the neutron star moment of inertia in units of 10^{45} g cm^2.

It has been a common practice to parameterize the spin-down of a rotation-powered pulsar by a power-law decrease of its rotational frequency, $\dot{\nu}(t) = -C\nu^n$, where $\dot{\nu}$ is the spin frequency derivative, C is a proportionality constant, and n is the so-called braking index. Theoretically, n can be computed for each given energy loss mechanism. In addition, the numerical value of C depends on the intrinsic properties of the neutron star, such as moment of inertia and radius. Possible models for the loss mechanism of the rotational energy include dipole and higher multipole electromagnetic radiation, gravitational quadrupole radiation, and a pulsar wind (see, e.g., Manchester & Taylor 1977; Melatos 1997). In the standard model of rotating dipole in vacuum with pure magnetic braking, $n = 3$. If both C and n are assumed to be constant over time, then $n = \nu\ddot{\nu}/\dot{\nu}^2$ and measurements of the frequency and its derivatives provide a braking index at a given epoch, possibly allowing us to discriminate between models of pulsar spin-down.

For most young pulsars (age less than 10^4 yr) an accurate determination of the braking index is a challenge because of difficulty in measuring the second derivative. For example, young pulsars tend to display varying degrees of timing irregularities, including "timing noise," a stochastic fluctuation of the pulse phase, and sudden spin-up events, known as "glitches," typified by discontinuous changes in spin frequency and its time derivatives. Furthermore, the typical magnitude of the second derivative is such that its effect on the pulse arrival times becomes measurable only over timescales of hundreds of days to several years. Braking indexes have so far been reported for five pulsars, all of which are below 3: 2.51 ± 0.01 for the Crab pulsar (Lyne, Pritchard, & Smith 1988), 2.837 ± 0.001 for PSR B1509−58 (Kaspi et al. 1994), 1.4 ± 0.2 for the Vela pulsar (Lyne et al. 1996), 2.91 ± 0.05 for PSR J1119−6127 (Camilo et al. 2000), and several inconsistent values ranging from 2.0 to 2.8 for PSR B0540−69 (see Boyd et al. 1995 and Eikenberry, Fazio, & Ransom 1998 for compilations of past measurements). The apparently inconsistent values for PSR B0540−69 have been obtained by combining data sets across different experiments at different wavelengths or over long time intervals that could not be phase-linked. Any glitches between observations could not have been properly taken into account.

In this Letter, we report a new and definitive measurement of the braking index of PSR B0540−69 using a phase-connected ephemeris obtained from a series of X-ray observations spanning more than 1 yr. These measurements provide accurate values for ν, $\dot{\nu}$, $\ddot{\nu}$, and the braking index n. In particular, for the first time a glitch has been observed from this pulsar that causes discontinuous changes in both ν and $\dot{\nu}$.

2. OBSERVATIONS

The data for this Letter were obtained with the Proportional Counter Array (PCA) on board NASA's *Rossi X-Ray Timing Explorer* (*RXTE*) for the purpose of monitoring the 16 ms pulsar PSR J0537−6910 (Marshall et al. 1998), located 22′ from PSR B0540−69, which still fits easily within the *RXTE* 1° (FWHM) field of view. The exact observation epoch and time duration

[1] Laboratory for High Energy Astrophysics, Goddard Space Flight Center, Greenbelt, MD 20771; william.w.zhang@gsfc.nasa.gov, francis.e.marshall@gsfc.nasa.gov.

[2] Columbia Astrophysical Laboratory, Columbia University, 550 West 120th Street, New York, NY 10027; eric@astro.columbia.edu.

[3] Los Alamos National Laboratory, CCS-3, MS B256, Los Alamos, NM 87545; jon@lanl.gov.

[4] Department of Astronomy, University of Massachusetts, B-524, Lederle Graduate Research Tower, Amherst, MA 01003; wqd@hnr.astro.umass.edu.

of each pointing have been optimized for phase-linking the pulses from PSR J0537−6910 and were easily sufficient for phase-linking PSR B0540−69, which is both slower and brighter than PSR J0537−6910.

The PCA is sensitive to X-rays in the 2–60 keV band, with a spectral resolution $E/\Delta E \sim 18\%$ at 6 keV. Each X-ray is time-tagged with a 1 μs accuracy with respect to the spacecraft clock, which is maintained to UTC to better than 100 μs. The background count rate consists of contributions from unrejected charged particles, which have a flat energy spectrum, and diffuse background X-rays, which have a power-law energy spectrum. In addition, the nearby and much brighter X-ray source LMC X-1 contributes substantially to the overall count rate. In order to optimize the ratio of pulsed signal to unpulsed background, given the Crab-like energy spectrum of PSR B0540−69 (Mineo et al. 1999), we selected only the events from the top layer of the PCA detectors with pulse-height channels between 5 and 50, which correspond approximately to the energy range of 2–15 keV.

3. DATA ANALYSIS AND RESULTS

We first converted the arrival time of each photon recorded by the *RXTE* satellite to the corresponding time at the solar system barycenter using the source position $\alpha = 5^{\rm h}40^{\rm m}10\overset{\rm s}{.}95$, $\delta = -69°19'55\overset{''}{.}1$ (J2000.0) (Caraveo et al. 1992). We then performed a fast Fourier transform (FFT) on each observation to determine a preliminary mean pulsar frequency (without accounting for any $\dot{\nu}$) and folded each observation into 20 phase bins over a range of frequencies centered on the peak FFT frequency. We used the parameters corresponding to the maximum $\chi^2_{\rm max}$ to determine a pulse time of arrival (TOA) for each observation. The standard deviation (or 1 σ error) for the frequency measurement was computed from the two frequencies on either side of the maximum $\chi^2_{\rm max}$, which correspond to $\chi^2_{\rm max} - 1$. Table 1 lists the relevant parameters for each observation and the corresponding measured pulse frequencies and TOA.

A linear fit to the measured pulse frequency as a function of MJD with $t_0 =$ MJD 51,197.000000 resulted in $\nu_0 = 19.80244322(25)$ Hz and $\dot{\nu}_0 = -1.8773(2) \times 10^{-10}$ Hz s^{-1} and a χ^2 of 60.6 for 44 degrees of freedom, where the numbers in parentheses represent 1 σ errors on the last digits. A quadratic fit was not needed and did not substantially improve the χ^2 per degree of freedom. We then used these ν_0 and $\dot{\nu}_0$ as our starting parameters to link the measured TOAs. The iterative procedure was as follows: (1) we started with the first four points to compute the predicted TOAs using ν_0 and $\dot{\nu}_0$; (2) we then took the difference between the measured and the expected TOAs as a function of MJD; (3) we performed a linear (or quadratic when necessary) fit to the differences in the TOAs versus MJD; (4) we derived corrections to ν_0 and $\dot{\nu}_0$ from the fit parameters; and finally (5) we then added the next data point and repeated the above procedure with the new values for ν_0 and $\dot{\nu}_0$ (and $\ddot{\nu}_0$ when necessary) until all data points had been included.

Figure 1 shows the final residuals, i.e., measured minus expected TOAs as a function of MJD. It turned out that it was not possible to link the entire set of TOAs with one set of ν_0, $\dot{\nu}_0$, and $\ddot{\nu}_0$. The pulsar suffered a glitch that was too small to show up directly in frequency but large enough to show up in the analysis of the TOAs. In order to ensure that the parameters derived with the above procedure are indeed the best and unique ones, we performed an exhaustive grid search in the three-dimensional space spanned by ν_0, $\dot{\nu}_0$, and $\ddot{\nu}_0$ with a step size in each of the three axes corresponding to 0.001 cycles. We included the first 16 observations to derive ephemeris 1 and observations 17–45 for ephemeris 2. These searches showed unambiguously that the parameters derived from our fits are indeed optimal with respect to the data set in that they minimize the χ^2 constructed from the difference between the measured and expected TOAs. There were many local minima that correspond to different parameters, but their χ^2-values are substantially larger than the minimum corresponding to the parameters derived from the above fit. Since data points 1–16 did not cover sufficient length in time so as meaningfully to constrain $\ddot{\nu}$, we used the $\ddot{\nu}$ derived from data points 17–45 for phase-linking. The global χ^2 minimum was approximately 5 per degree of freedom using the phase errors in Table 1. The final parameters and their corresponding errors are listed in Table 2. Note that the error for each parameter corresponds to the value that causes a change of $\Delta\chi^2 = 5$ from the true minimum when the χ^2 is minimized with respect to other parameters. In addition, the values of ν_0 and $\dot{\nu}_0$ for both ephemerides are

TABLE 1
PULSE PEAK TOA AND FREQUENCY MEASUREMENTS

Pointing	MJD	TOA (s)	Error (μs)	f (Hz)	Error (μHz)
1	51,197	9714.568504	312	19.80244199	0.38
2	51,198	26514.568395	454	19.80242174	2.95
3	51,200	48178.579829	526	19.80238934	3.47
4	51,206	59938.596437	435	19.80228181	3.03
5	51,220	35811.591565	455	19.80206455	2.69
6	51,237	24840.613416	500	19.80178861	2.42
7	51,253	4093.569518	406	19.80153397	0.78
8	51,254	733.580443	599	19.80151220	5.63
9	51,256	35886.568897	490	19.80147588	3.37
10	51,262	57377.602114	443	19.80138993	5.93
11	51,276	21671.602338	489	19.80115542	2.31
12	51,294	8304.570461	538	19.80086984	3.83
13	51,310	40888.611936	320	19.80060268	0.48
14	51,311	49177.592509	515	19.80059598	7.53
15	51,313	31178.584230	472	19.80055634	0.82
16	51,319	24524.597526	602	19.80046129	5.53
17	51,333	642.613976	608	19.80023518	2.99
18	51,342	80261.583293	442	19.80007535	2.50
19	51,349	17271.594834	448	19.79997620	2.83
20	51,366	3467.595263	325	19.79970215	0.65
21	51,367	3419.589460	417	19.79968537	2.71
22	51,369	27073.602006	458	19.79964401	3.55
23	51,375	44266.599721	427	19.79954705	3.25
24	51,389	13394.611715	452	19.79932976	3.51
25	51,405	76418.593236	437	19.79906016	2.76
26	51,423	22069.593972	332	19.79877325	0.30
27	51,425	66581.567332	323	19.79873374	1.62
28	51,432	4659.588230	399	19.79862202	3.40
29	51,462	69445.562182	440	19.79813066	1.36
30	51,480	23788.607873	299	19.79784807	0.20
31	51,481	22460.614450	451	19.79782856	5.73
32	51,483	23723.600730	369	19.79779904	1.90
33	51,489	54680.580130	447	19.79769697	2.31
34	51,504	2593.592806	519	19.79746406	1.71
35	51,519	81787.607271	416	19.79720142	3.47
36	51,536	85141.571535	441	19.79693308	2.64
37	51,537	36245.578151	300	19.79692150	0.22
38	51,546	54292.593408	435	19.79677326	2.75
39	51,560	25794.592166	450	19.79655572	3.53
40	51,576	49682.614931	449	19.79628170	3.25
41	51,589	34260.604618	459	19.79607262	2.98
42	51,616	21132.570140	361	19.79564384	2.19
43	51,628	60738.564796	311	19.79544100	0.56
44	51,629	8834.594404	390	19.79543520	0.33
45	51,631	3187.562038	343	19.79540322	0.64

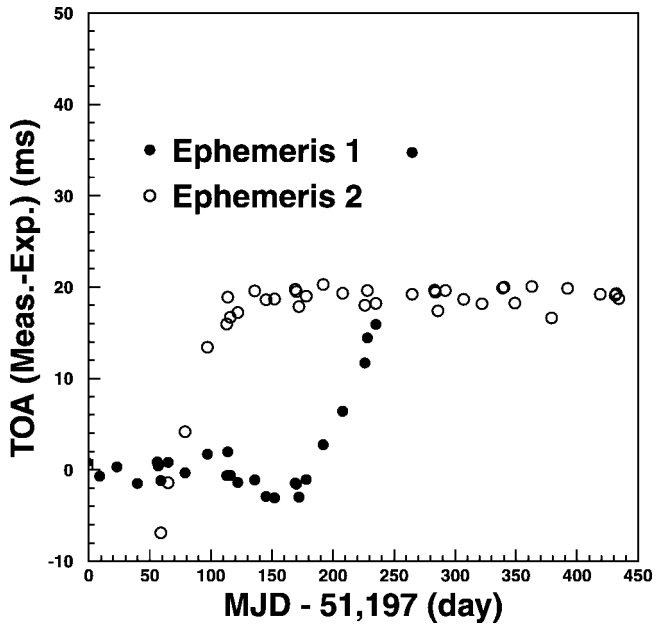

FIG. 1.—Difference between the measured pulse arrival time and the expected arrival time as a function of MJD for the 46 observations analyzed. The two sets of symbols correspond to the expectations from the two ephemerides in Table 1. The typical statistical phase error is 0.5 ms, which is smaller than the symbols.

those at the epoch of the first observation, i.e., 9714.568 s on MJD 51,197. We finally fitted the data points in Figure 1 with two polynomials of the third order to find that the glitch occurred on MJD 51,325 ± 45 (90% CL error). The large uncertainty on the exact epoch of the glitch was due to the small magnitude of the glitch. Propagating the parameters in Table 2 to this epoch, we found that the glitch was characterized by a change in frequency and frequency derivative, respectively: $\Delta\nu/\nu = (1.90 \pm 0.05) \times 10^{-9}$ and $\Delta\dot{\nu}/\dot{\nu} = (8.5 \pm 0.5) \times 10^{-5}$.

Given the magnitudes of the $\Delta\nu/\nu$ and $\Delta\dot{\nu}/\dot{\nu}$, it appears somewhat arbitrary whether to call such an occurrence a glitch or simply pulsar phase noise. To help answer this question, we also fitted the entire data set with polynomials of higher orders. For example, a sixth-order polynomial could fit the entire data set with a reduced χ^2 of 11 per degree of freedom, to be compared with 5 per degree of freedom in the case of two separate third-order polynomials. In particular, in comparison with other pulsars, we did not expect our data set to be of sufficient length to allow meaningful measurements of, or constraints on, higher time derivatives of the frequency. Given these considerations, we conclude that the characterization of the TOA with two separate third-order polynomials is physically warranted, and as such the observed phenomenon is a small, but genuine, glitch in both ν and $\dot{\nu}$.

4. COMPARISON WITH PREVIOUS MEASUREMENTS

There are a number of frequency measurements of PSR B0540−69 in the literature. The frequency ephemerides that were derived from substantial amounts of data are those of Boyd et al. (1995), Eikenberry et al. (1998), and Deeter, Nagase, & Boynton (1999). Extrapolating the frequency ephemeris of Boyd et al., which was derived from data covering the years from 1979 to 1993, to the time period of the observations in Table 1, consistently overpredicts our measured frequencies by tens of microhertz. The frequency ephemeris of Deeter et al. (1999), which was derived from data covering the years from 1985 to 1991, gives predictions typically within a few microhertz of the observed ones, which is comparable to the uncertainties of our frequency measurements. This serves to accentuate the fact that frequency measurements alone cannot accurately constrain pulsar parameters such as $\dot{\nu}$ and $\ddot{\nu}$.

Our measured braking index is significantly lower than those reported in the literature previously (see Boyd et al. 1995 for a compilation and a comprehensive analysis of all the frequency measurements up to 1995): 1.81 ± 0.07 versus 2.28 ± 0.02 (Boyd et al. 1995) and 2.0799 ± 0.00027 (Deeter et al. 1999). Eikenberry, Fazio, & Ransom (1998) analyzed *ROSAT* data spanning a 3 yr period and concluded that PSR B0540−69 has intrinsic timing noise that prevents accurate and consistent measurements of its braking index. They quoted an $n = 2.5^{+0.6}_{-0.7}$ whose errors are dominated by timing noise. All those previous measurements explicitly assumed that the pulsar had not suffered any glitches during the observation intervals. The presence of a glitch in our data set, and the many inconsistent values reported for the braking index, strongly indicate that there may have been many other glitches in the timing history of B0540−69. In particular, when we combine the data points in Table 1 of Boyd et al. (1995) with the 45 frequency measurements in Table 1 of this work, we obtain a braking index of 2.103 ± 0.005, significantly lower than 2.28 ± 0.02. This is a clear indication of the fact that, if no phase-link can be established among different observations, glitches can prevent an accurate determination of the secular $\dot{\nu}$ and $\ddot{\nu}$ of pulsars. For example, if a pulsar glitches at a rate R with only a frequency jump for each glitch and the sampling of the frequency measurements is such that there are initially several closely spaced observations that allow accurate determinations of ν and $\dot{\nu}$ but not $\ddot{\nu}$, another observation separated by a long time T from those initial observations would allow an estimate for $\ddot{\nu}$. It is inevitable that one would attribute the effect of any glitches between the two sets of observations to $\ddot{\nu}$ so as to overestimate

TABLE 2
EPHEMERIS FOR PSR B0540−69 DERIVED FROM THE DATA SET[a]

Ephemeris	ν_0 (Hz)	$\dot{\nu}_0$ ($\times 10^{-10}$ Hz s^{-1})	$\ddot{\nu}_0$ ($\times 10^{-21}$ Hz s^{-2})	n
1	19.802442043(5)	−1.878013(9)	3.23[b]	...
2	19.802442257(12)[c]	−1.878173(9)	3.23(12)	1.81 ± 0.07

[a] The t_0 is MJD (barycentric dynamic time) 51,197.11243713, which corresponds to the time of the first observation as listed in Table 1.

[b] The data set is not of sufficient length to meaningfully constrain $\ddot{\nu}$. We fixed $\ddot{\nu}$ to the value obtained for ephemeris 2.

[c] The larger error for ephemeris 2 is due to the fact that the three parameters are highly correlated.

the $\ddot{\nu}$ by $\sim 2R\Delta\nu/T$. In other words, the amount of overestimate is proportional to glitch rate R. On the other hand, if the sampling of the frequency measurements is not so sparse, the effects of glitches may be attributed to both $\dot{\nu}$ and $\ddot{\nu}$. Real situations with any pulsar are likely to be complicated by more factors, such as a $\dot{\nu}$ that can also change discontinuously during glitches. Given the above simple scenario, many glitches (~ 1 yr^{-1}) of the magnitude we have observed could have certainly caused the much larger and inconsistent measurements of the braking index reported in the literature. While the glitch rate of PSR B0540−69 is not known, rates from other Crab-like pulsars, such as PSR J537−6910 (one every few months; Marshall et al. 2000) and Vela (nine glitches in 25 yr; Lyne et al. 1996), certainly indicate that it is possible that PSR B0540−69 can have an average glitch rate of one per year. Since our measurements come from phase-linked data sets, they provide the true secular braking index.

It is interesting to note that our measured braking index agrees reasonably well with solution 3, i.e., $\nu_0 = 19.850286416(3)$ Hz, $\dot{\nu}_0 = -1.887654(3) \times 10^{-10}$ Hz s^{-1}, $\ddot{\nu}_0 = 3.30(3) \times 10^{-21}$ Hz s^{-2}, and $n = 1.84(2)$ at MJD 8256.500000128, presented in Gouiffes, Finley, & Ögelman (1992). They analyzed their self-contained data set of 15 measurements sampled over the period from 1989 January to 1991 April and arrived at three sets of ν, $\dot{\nu}$, and $\ddot{\nu}$ that fit their data equally well. They eventually chose solution 1 as most likely, based on an earlier *Ginga* measurement extrapolated to the epoch of their observations (Nagase et al. 1990; see also Deeter et al. 1999), assuming there had not been any glitches in the intervening time span. Given our current phase-linking measurement and the fact that this pulsar does indeed glitch, we conclude that their premise for choosing solution 1 was not valid and that solution 3 is most likely correct.

If we consider the reasonable agreement between our measurement and solution 3 with $n = 1.84 \pm 0.01$ of Gouiffes et al. (1992), we can derive a value for $\nu \ldots = -(2 \pm 1) \times 10^{-31}$ Hz s^{-3}. On the other hand, $\nu \ldots$ can also be computed from the formula $\nu \ldots = n(2n - 1)\dot{\nu}^3/\nu^2$ to be -0.82×10^{-31} Hz s^{-3}. The agreement within the albeit large error indicates that the power-law slowdown is an adequate description for this pulsar.

5. DISCUSSION

The glitch from PSR B0540−69 is small in terms of the magnitudes of $\Delta\nu/\nu$ and $\Delta\dot{\nu}/\dot{\nu}$, compared with glitches from other Crab-like pulsars (Lyne & Graham-Smith 1998). There is no indication that the pulsar is recovering from the glitch; i.e., there is no decay of the excess frequency over time following the glitch. Our data set is not sufficient for us to further characterize the properties of the glitch. Given that only one glitch was observed in 434 days and assuming that glitch occurrence obeys the Poisson distribution, we conclude that, in order to have either one or zero glitches 90% of the time, the underlying average number of glitches during the same period cannot be more than 3.89. This translates into a 90% CL PSR B0540−69 glitch rate of no higher than 3.3 times yr^{-1}. Given the short duration of our data set, it is not clear whether glitches like the one observed here can account for the timing noise referred to by Eikenberry et al. Continued monitoring of this pulsar over several years with the *RXTE* is needed to resolve this question.

The timing noise, or residual phase, as seen in Figure 1 is qualitatively comparable to those in Deeter et al. (1999). Using the residual phases for observations 1–16 from ephemeris 1 and observations 17–45 from ephemeris 2, we calculate the rms residual to be 1 ms, which is theoretically the TOA measurement uncertainty and the true pulsar timing noise added in quadrature. Given the fact that our measurement uncertainty is typically 0.5 ms, we conclude that the residual is dominated by pulsar timing noise, which is of the order 0.85 ms.

Of the four young pulsars whose braking indexes have been measured, the Vela pulsar and PSR B0540−69 have particularly small ones. As a matter of fact, Vela's 1.4 ± 0.2 and PSR B0540−69's 1.81 ± 0.07 are not much different from each other, given the measurement errors. These values are significantly smaller than 3, which is expected from pure magnetic dipole braking. This indicates that there are processes other than, or in addition to, magnetic dipole radiation that play important roles in the loss of pulsar rotational energy. This low braking index, together with the evidence for synchrotron radiation in the nebula around the pulsar, indicates that particle acceleration is an important mechanism through which a magnetized neutron star loses its rotation energy.

We wish to thank V. Kaspi for her suggestions that have helped us improve this Letter. The research of E. V. G. is supported by NASA LTSA grant NAG5-7935. This research has made use of data obtained through the High Energy Astrophysics Science Archive Research Center Online Service, provided by the NASA/Goddard Space Flight Center.

REFERENCES

Boyd, P. T., et al. 1995, ApJ, 448, 365
Camilo, F., Kaspi, V. M., Lyne, A. G., Manchester, R. N., Bell, J. F., D'Amico, N., McKay, N. P. F., & Crawford, F. 2000, ApJ, 541, 367
Caraveo, P. A., Bignami, G. F., Mereghetti, S., & Mombelli, M. 1992, ApJ, 395, L103
Deeter, J. E., Nagase, F., & Boynton, P. E. 1999, ApJ, 512, 300
Eikenberry, S. S., Fazio, G. G., & Ransom, S. M. 1998, ApJ, 492, 754
Gouiffes, C., Finley, J. P., & Ögelman, H. 1992, ApJ, 394, 581
Kaspi, V. M., Manchester, R. N., Siegman, B., Johnston, S., & Lyne, A. G. 1994, ApJ, 422, L83
Lyne, A. G., & Graham-Smith, F. 1998, Pulsar Astronomy (Cambridge: Cambridge Univ. Press), 64
Lyne, A. G., Pritchard, R. S., Graham-Smith, F., & Camilo, F. 1996, Nature, 381, 497
Lyne, A. G., Pritchard, R. S., & Smith, F. G. 1988, MNRAS, 233, 667
Manchester, R. N., Mar, D. P., Lyne, A. G., Kaspi, V. M., & Johnston, S. 1993, ApJ, 403, L29
Manchester, R. N., & Taylor, J. H. 1977, Pulsars (San Francisco: Freeman)
Marshall, F. E., Gotthelf, E. V., Middleditch, J. Wang, Q. D., & Zhang, W. 2000, in ASP Conf. Ser. 202, Pulsar Astronomy—2000 and Beyond, ed. N. Kramer, N. Wex, & R. Wielebinski (San Fransisco: ASP), 335
Marshall, F. E., Gotthelf, E. V., Zhang, W., Middleditch, J., & Wang, Q. D. 1998, ApJ, 499, L179
Melatos, A. 1997, MNRAS, 288, 1049
Middleditch, J., & Pennypacker, C. 1985, Nature, 313, 659
Mineo, T., Cusumano, G., Massaro, E., Nicastro, L., Parmar, A. N., & Sacco, B. 1999, A&A, 348, 519
Nagase, F., Deeter, J., Lewis, W., Dotani, T., Makino, F., & Mitsuda, K. 1990, ApJ, 351, L13
Seward, F. D., Harnden, F. R., Jr., & Helfand, D. J. 1984, ApJ, 287, L19